19th Brazilian Congress of Thermal Sciences and Engineering
November 6th–10th, 2022, Bento Gonçalves - RS - Brazil

ENC-2022-0446
EXPERIMENTAL INVESTIGATION OF THE INFLUENCE ON THE WALL TEMPERATURE ON INORGANIC SCALE DEPOSITION IN PIPES

Gabriel Siqueira Machado
Eric Claro Dittrich
Pedro Silva Petindá
Instituto Alberto Luiz Coimbra de Pós-Graduação e Pesquisa em Engenharia - COPPE - Departamento de Engenharia Mecânica, Universidade Federal do Rio de Janeiro - UFRJ, CEP 21941-914, Rio de Janeiro, Brazil
gabriel.machado@mecanica.coppe.ufrj.br
ericclaro@poli.ufrj.br
pedro.petinda@poli.ufrj.br
Gustavo Luiz Campos Pires
Instituto de Geociências , Universidade Federal do Rio de Janeiro - UFRJ, CEP 21941-916, Rio de Janeiro, Brazil
g.pires@geologia.ufrj.br
Juliana Braga Rodrigues Loureiro
Instituto Alberto Luiz Coimbra de Pós-Graduação e Pesquisa em Engenharia - COPPE - Departamento de Engenharia Mecânica, Universidade Federal do Rio de Janeiro - UFRJ, CEP 21941-914, Rio de Janeiro, Brazil
jbrloureiro@mecanica.coppe.ufrj.br

Abstract. *Calcium carbonate scale formation is a recurring problem in oil exploration in the Brazilian pre-salt. This phenomenon occurs with greater severity in heat exchangers located on the top side of oil platforms, as the solubility of calcium carbonate is inversely proportional to temperature. The objective of this work is to experimentally investigate the influence of a local wall temperature increase on the deposition of inorganic scale inside pipes. The experimental apparatus is an open-circuit flow loop, which consists of a 65 meter-long pipe, with an internal diameter of 11 mm, equipped with flowmeters and pressures transducers. The working fluid is a mixture of two incompatible brines. At the end of the pipe, a 0.43m heated section is installed, with hot fluid flowing in the annular section and the brine mixture flowing through the inner-tube, in a counter-current configuration. Along the pipe, including in the heated section, removable sections allow the measurement of the mass and thickness of the deposited material, as well as morphological analysis from images obtained from scanning electron microscopy (SEM). Results indicate that the higher wall temperature had a considerable effect on the mass and thickness of calcium carbonate scaling, as well as on the structure of the material formed. It was observed an increase of up to 240% in mass and 175% in thickness of the scaling produced in the heated pipe wall when compared to scaling formed in upstream locations. Moreover, it was noted that the type of deposition changed under the influence of the heated wall, which also caused the appearance of crystal polymorphs in the heated section not observed in removable sections further upstream.*

Keywords: *Scale formation, Wall temperature, Heated pipe, Scanning Electron Microscope, Calcium Carbonate*

1. INTRODUCTION

The prevention of formation of calcium carbonate ($CaCO_3$) scale formation at various stages of oil production is one of the main challenges of the Brazilian pre-salt exploration. The inorganic deposition in pipes, separators and valves severely reduces production rates, what can lead to unscheduled stoppage and severe economic consequences. According to Andritsos and Karabelas (2003), there are three main causes for calcium carbonate deposits to occur: increased salt concentration, loss of CO_2 from the solution (resulting in an increase solution pH) or increased temperature of the solution. The latter factor results in heat exchangers being a critical equipment for scaling formation, since calcium carbonate solubility decreases with increasing temperature (Brečević and Nielsen, 1989) and (Weyl, 1959).

According to Gargoum (2018), six calcium carbonate polymorphs are known. Three of them, known as calcite, vaterite and aragonite, are the anhydrous forms, considered more stable forms. Another two, known as calcium carbonate monohydrate and ikaite (or calcium carbonate hexa-hydrate), are the hydrated forms which are less stable than the other

three. The sixth and final phase is amorphous calcium carbonate (ACC), which is the least stable of all (Al Omari *et al.*, 2016).

The mechanism of polymorphic transformation of calcium carbonate is discussed by Ogino *et al.* (1990). He shows that the scaling formation proceeds from the dissolution of less-stable polymorphs and the growing of calcite according to Ostwald's step rule. This rule says that if a reaction can result in several products, it is not the most stable state, with the least amount of free energy that will initially be obtained, but the least stable state, i.e., closest to the original state in energy (Van Santen, 1984). The kinetics of this mechanisms is highlighted by Rodriguez-Blanco *et al.* (2011) and Bots *et al.* (2012), which shows that the transformation pathway is from an amorphous calcium carbonate (ACC) via vaterite to calcite, the most stable polymorph.

There is already evidence in the literature that bulk temperature influences the type of $CaCO_3$ polymorphs formed at the wall. Andritsos *et al.* (1996) studied the formation of $CaCO_3$ scaling in tube walls for varying fluid temperature. While calcite was the predominant polymorph at experiments conducted at 23°C, aragonite was kinetically stabilized at higher temperatures of 42°C.

The stabilization of aragonite at higher temperatures can be explained by two factors: the inverse solubility of calcium carbonate and the ionic activity product (IAP). Weyl (1959) shows that the solubility of calcium carbonate also drops with increasing aqueous carbon dioxide content, since the solubility of carbon dioxide is also inverse with increase temperature. Ogino *et al.* (1990) and Kawano *et al.* (2009) shows that IAP decreases with the increase of temperature along the time. Furthermore, they show that the more stable the polymorph, the lower the ionic activity. Therefore, the higher the temperature, the higher the IAP and the lower the solubility of the solution, resulting in stabilization of polymorphs that would be less stable under ambient conditions.

Figure 1 shows the physical processes of the scale formation and the types of deposition. When the particle nucleates and grows on the surface of the wall, it is called ionic deposition. This type of deposition is characterized by the well-structured and organized form of crystal growth. When this particle does this process on the bulk of the solution and then it is deposited on the surface, is particle deposition. This type of deposition is characterized by single crystals of calcium carbonate arranged chaotically and without a growing structure.

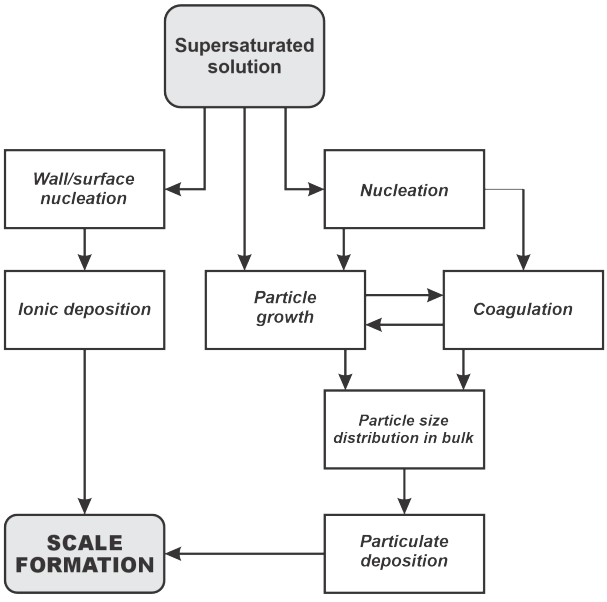

Figure 1: Physical processes of scale formation. Adapted from (Kostoglou and Karabelas, 1998)

The objective of this work is to experimentally investigate the influence of a local wall temperature raise on the deposition of inorganic scale inside pipes.

2. EXPERIMENTAL METHODOLOGY

2.1 Experimental apparatus

The Multipurpose Flow Loop is installed at the Interdisciplinary Center for Fluid Dynamics of the Federal University of Rio de Janeiro. The essential schematic of the rig is depicted in Fig. 2.

Two large reservoirs with volumes of 5.0 m^3, which are open to the atmosphere (at sea level), were used to store aqueous solutions of calcium chloride ($CaCl_2$) and sodium bicarbonate ($NaHCO_3$). The solutions were prepared with a

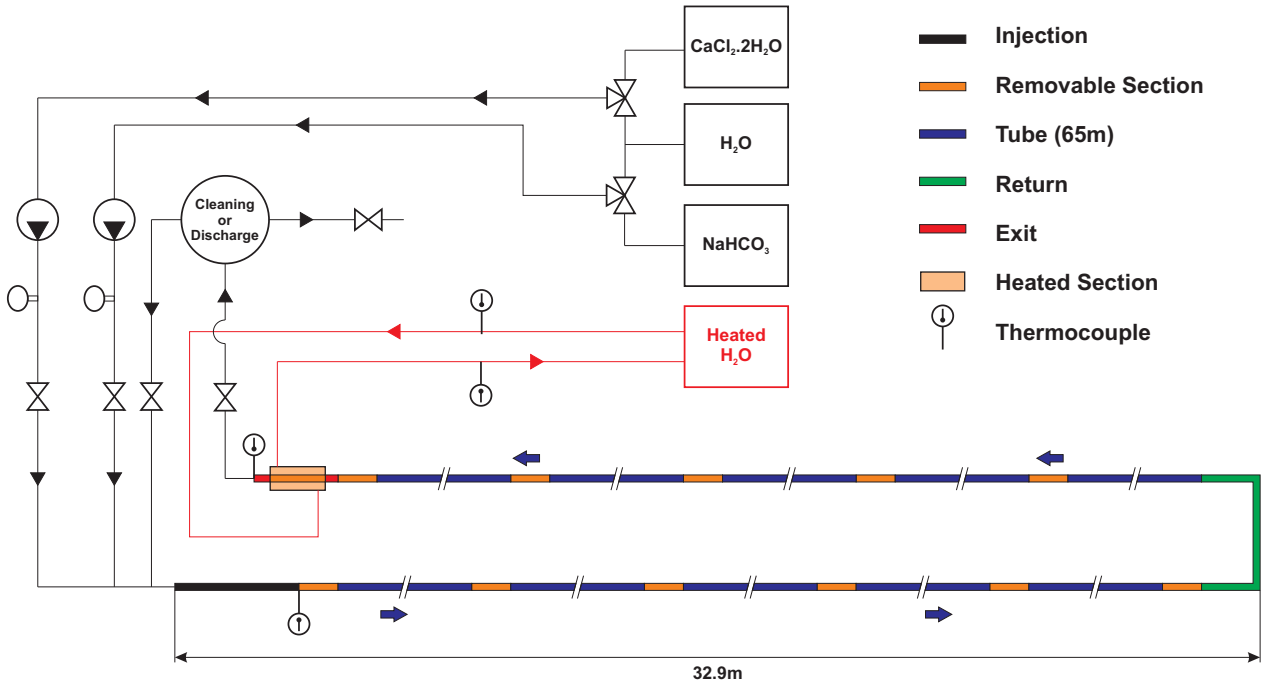

Figure 2: Layout of the experimental setup.

concentration of 150 mM (0.150 mol/L) of sodium bicarbonate and 56 mM (0.056 mol/L) of calcium chloride. Another reservoir with volume of 4.0 m^3 was used to store pH neutral potable water.

Particles with linear sizes smaller than 5 μm were removed from the fluid through the use of filters. The standard procedure to ensure test reproducibility is to assure the aqueous ionic solutions have reached pH equilibrium.

The ionic solutions were simultaneously pumped by two Netzsch progressive cavity pumps and mixed at the pipe inlet at a 1:1 ratio. The flowrate of the individual brines is monitored by two electromagnetic flow meters (Endress+Hauser Proline Promag E 100) positioned downstream of the pumps. The resulting flow then runs through a 65m-long stainless-steel pipe with a constant inner diameter of 11 mm, being discharged at the outlet at ambient pressure. The entire system is submitted to ambient temperature, and flow temperature is monitored by temperature probes at the inlet and outlet of the rig.

The hot fluid used to increase the wall test section consists of water, stored in an 8m^3 tank equipped with two 30kW electrical resistances. Fluid temperature in the tank is raised to 80°C and kept constant at this level by a closed-loop control. The hot water is pumped though the heated section in a counter-current configuration, entering and exiting the annular in the radial direction. The hot fluid entry and exit temperatures are continuously monitored by thermocouples.

2.2 Measurement techniques

The heated wall section consists of a 0.45m-long double-pipe configuration, as sketched in Fig. 3a, with the brine mixture flowing through the internal pipe and the hot fluid in its annular region in a counter-current flow. It is located at the end of the flow loop just before its exit. The inner pipe is the same used in the flow loop. This configuration imposes a step change of the inner-tube wall temperature as the flow enters the section.

Along the pipe, eleven removable test sections allow the measurement of the mass and thickness of the deposited material, as well as polymorphic, morphological and textural analysis in a scanning electron microscope (SEM). The removable section contains two parts as shown in Fig. 3b: the weighing section and the SEM section, which have the same diameter of the main tube and are 120 mm and 20 mm long, respectively. After each experiment the removable sections are set to dry for 24h before being weighted.

Absolute pressure is measured along the pipe after each removable section. Therefore, the rig contains a total of eleven measurement points which are distant from each other by approximately 6 m. The first pressure point, located 7.7m from the inlet, is connected to a dedicated pressure transmitter providing constant data during the experiment. The remaining pressure points are connected to another pressure transmitter through a set of valves. Both transmitters are manufactured by Yokogawa (model EJA510E).

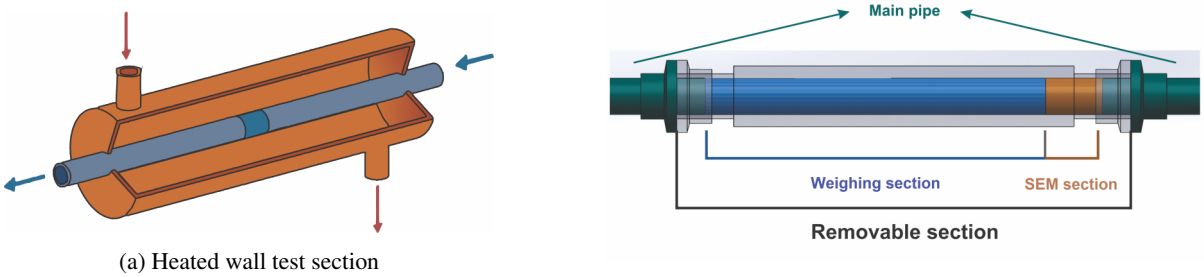

(a) Heated wall test section

(b) Removable test section.

Figure 3: Heated and removable test sections.

2.3 Test Matrix

Eight tests were performed, 3 of them with the heated section (one for each Reynolds number) and five of them without the heated section for comparison and replica purposes. The test was carried out for three different flow rates given by 300, 450 and 600 L/h, corresponding to the Reynolds number range 11500 < Re < 22800. Table 1 shows the experimental matrix with the ID experiment, flow rate, Reynolds number and if the test was conduct with the heated section.

Table 1: Experimental matrix

ID experiment	Flow rate [L/h]	Reynolds number	Heated
01	300	11500	-
02	300	11500	-
03	300	11500	X
04	450	16900	-
05	450	16900	X
06	600	22800	-
07	600	22800	-
08	600	22800	X

3. RESULTS

3.1 Wall temperature

One key parameter necessary to characterize the scaling results in the heated section is the wall temperature of the inner tube, through which the mixture of brines is flowing. The device will introduce a radial temperature gradient between the bulk temperature to that on the wall. Close to the wall scaling will be formed at higher temperatures. For this experimental analysis, this quantity will be computed using double-pipe heat transfer coefficient estimations and temperature measurements of the brine mixture.

In order to compute T_{wall}, the inlet and outlet temperatures at the heated section of both cold and hot fluids are required. As can be seen in Figure 2, thermocouples placed in the setup measure directly the inlet and outlet temperatures of the hot fluid ($T1_{hot}$ and $T2_{hot}$), as well as at the outlet temperature of the inner tube ($T2_{cold}$). However, the inlet temperature of the brine mixture $T1_{cold}$ was not directly measured in order to avoid flow perturbations than could influence the $CaCO_3$ deposition in the inner tube walls. The inlet temperature of the brine mix is monitored only at the injection of the flow loop $T1_{cold,inj}$, which is located roughly 64m upstream of the heated section.

Therefore, the first step is to estimate a representative temperature variation over the pipe length until the brine mixture reaches the heated section inlet. This can be done by analyzing temperature data from experiments without heating. It can be seen from Fig. 4 that temperature rise in non-heated experiments vary between 0.4 and 0.9°C, whereas heated ones display a temperature variation of 3.15 to 3.55°C. Hence, a temperature rise ΔT_{pipe} between the pipe outlet and inlet of 0.65°C is considered to estimate the brine inlet temperature at the heated section $T1_{cold,exp}$.

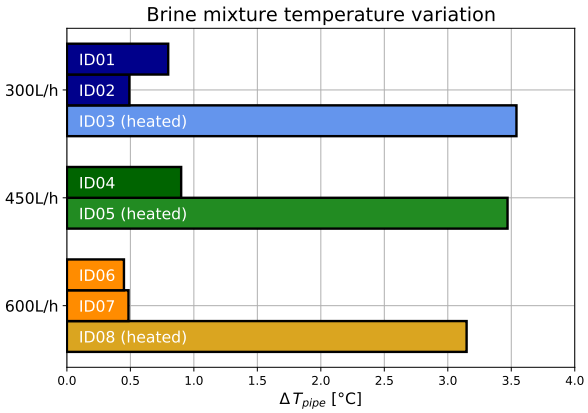

Figure 4: Temperature rise between flow loop inlet and outlet.

Table 2: Inlet and outlet temperatures for experiments with heated section, alongside wall temperature estimates.

Q [L/h]	300	450	600
$T1_{cold,inj}$ [°C]	26.74	26.63	26.54
$T1_{cold,exp}$ [°C]	27.39	27.28	27.19
$T1_{cold,alg}$ [°C]	27.30	27.42	27.20
$T2_{cold}$ [°C]	30.28	30.1	29.69
T_{wall} [°C]	55.26	55.23	55.07

The wall temperature is estimated by assuming that there are no heat losses, conductivity over the inner tube thickness is negligible and that brine mixture thermodynamic properties can be approximated by those of water for a given temperature. The heated section is discretized in 40 elements, as shown in Fig. 5. Due to the counter-current configuration, bulk temperatures of the first element annular and inner-tube are set to be $T1_{hot}$ and $T2_{cold}$, both directly measured quantities. The wall temperature T_{wall} and heat transfer coefficients on each element are determined iteratively using tube- and annular-side Nusselt number relations for turbulent flows from Taborek (1997). Then, the Effectiveness NTU method (Incropera *et al.*, 1996) is used to determine the outlet bulk temperatures of the first element, i.e., the inlet temperatures of the following element. At the end of the heated section, the algorithm estimates both $T2_{hot}$ and $T1_{cold,alg}$.

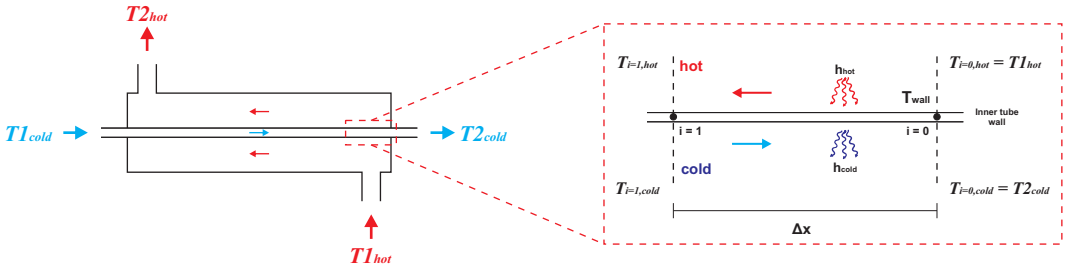

Figure 5: Calculation method for wall temperature.

In order to validate the numerical procedure, a comparison is made between the inlet brine temperature computed by the algorithm $T1_{cold,alg}$, and that estimated experimentally $T1_{cold,exp}$ obtained by adding ΔT_{pipe} to $T1_{cold,inj}$ (measured at the flow loop injection). This analysis is summarized in Table 2. There is clearly a very good agreement between both estimated $T1_{cold}$ temperatures. It can be seen that T_{wall} for the three cases lies consistently around 55°C.

3.2 Scaling

Since the heated and weighing test sections are different in length, the mass deposition was divided by the length of each one.

Figure 6 shows the results for each measured flow rate. It can be seen that normalized mass and thickness have a well-behaved profile until the heated section where the mass and thickness increase significantly. Comparing the results of the last four test sections, it can be seen that there was an increase in the mass deposition of almost 240% at Re = 11500, 110% at Re = 16900 and 170% at Re = 22800 for the heated section. These results indicate that the higher temperature of the wall favors the deposition rate. About the scale thickness comparison, there was an increase in the scale thickness of almost 175% at Re = 11500, 110% at Re = 16900 and 70% at Re = 22800 for the heated section.

Figure 7 shows the morphology of deposition. For the flow rate of 300 l/h, polycrystalline dendritic calcite appears (Fig. 7a). As the distance from the mixture point increases, the polymorphic structure changes, appearing vaterite on the top of deposition (Fig. 7b) as well as the type of deposition changes from ionic deposition to particulate deposition (Fig. 7c).

Along the pipe, it was observed that vaterite becomes more frequent. This result suggests that as the solubility of the solution decreases, vaterite cannot resolubilize and recrystallize into calcite, maintaining its structure. Figure 8 shows that

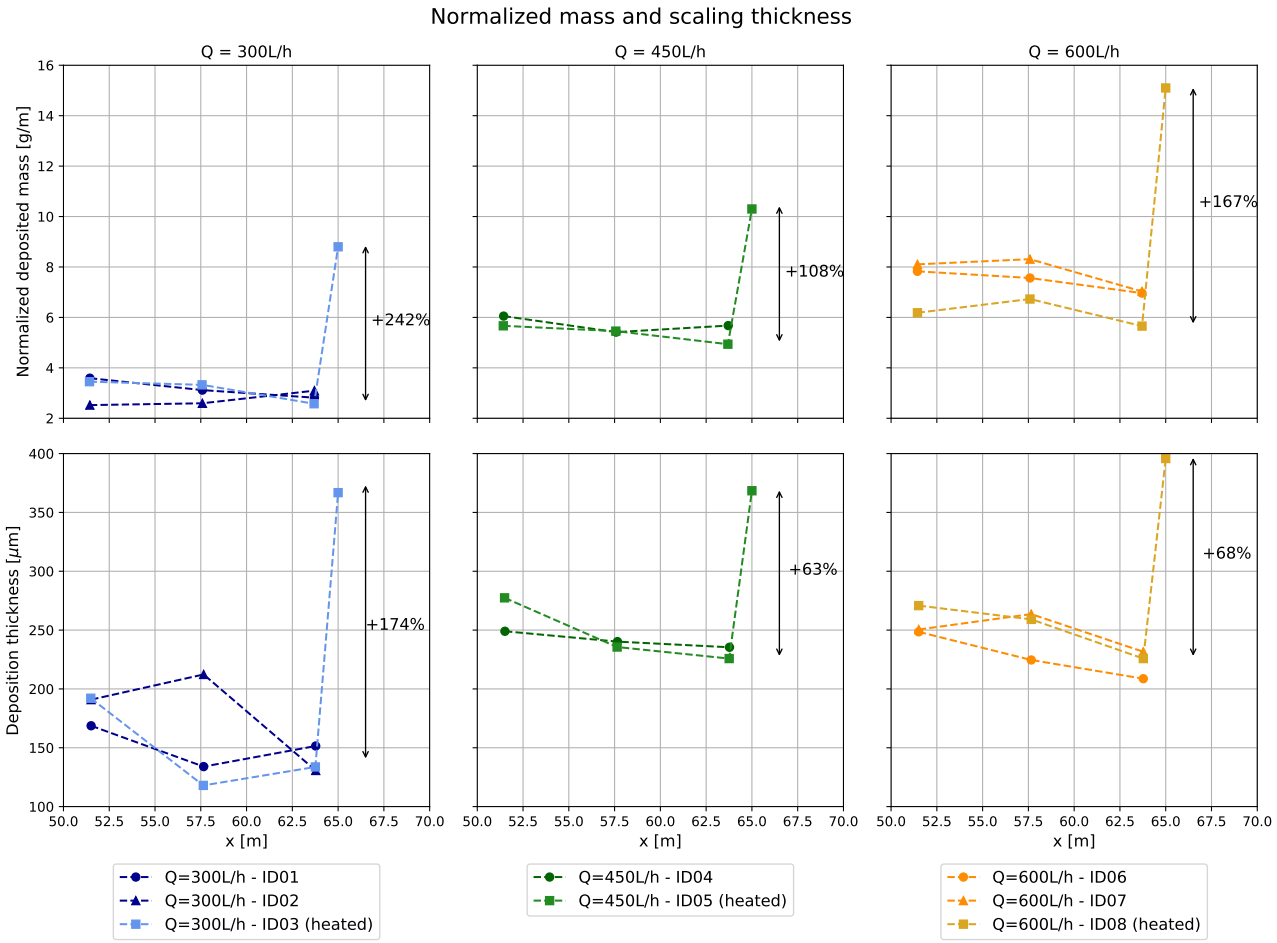

Figure 6: Scaling thickness and normalized mass at the end of the flow loop, for experiments with and without the heated section.

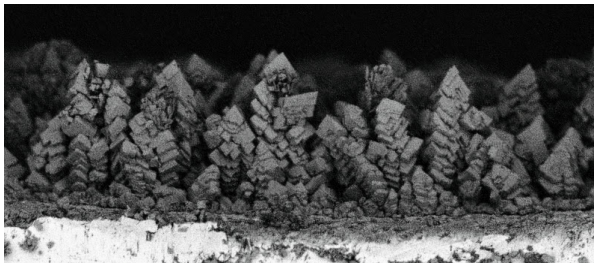

(a) Example of polycrystalline dendritic calcite (Re = 11500, x = 51.4m)

(b) Example of vaterite (Re = 11500, x = 51.4m)

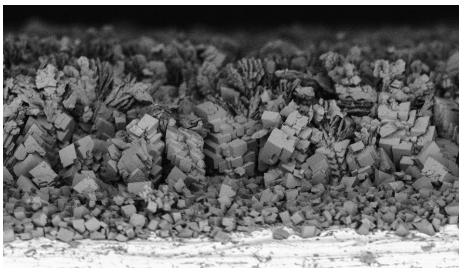

(c) Example of grainly calcite (Re = 16900, x = 63,7m)

Figure 7: Examples of morphology and deposition types

the recrystallization process begins at the edges of the vaterite structures.

In the SEM analysis, it is possible to see the presence of acicular aragonite that appears due to the increase of the wall temperature (Fig. 9a and Fig. 9b). Furthermore, it is also possible to see the other form of vaterite, the flake-like vaterite

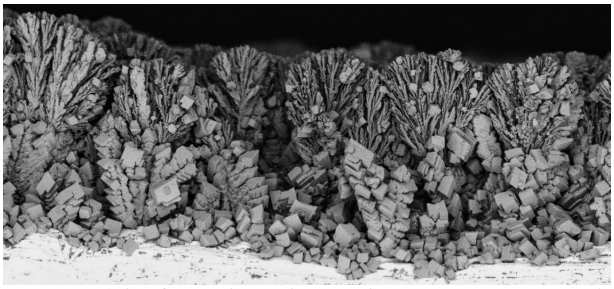

Figure 8: Calcite formation, via vaterite (Re = 22800, x = 51.4)

(Fig. 9c and Fig. 9d).

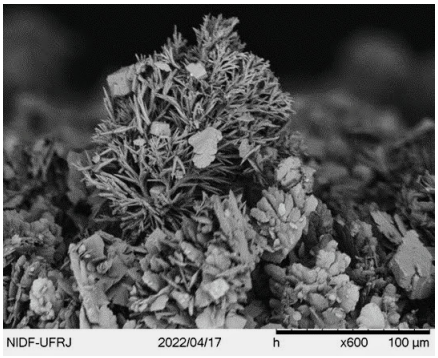

(a) Acicular aragonite.

(b) Acicular aragonite.

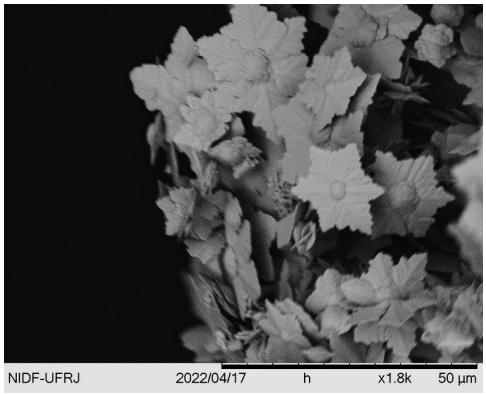

(c) Flake-like vaterite.

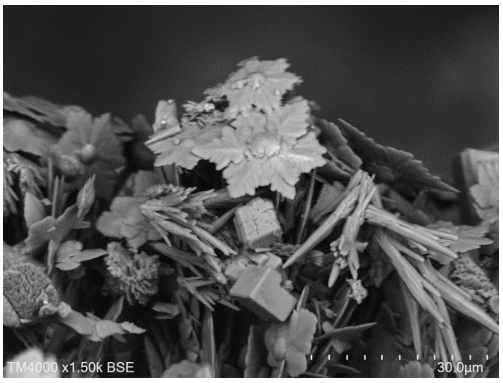

(d) Flake-like vaterite.

Figure 9: SEM images

This suggests that at high wall temperatures, the thermal boundary layer influences the solution that is close to the wall. As the solubility of the solution near to the wall decreases (due to the increase of the temperature), the vaterite resolubilizes and recrystallizes as aragonite, instead of calcite.

Figure 10 shows that the proportion between calcite and vaterite also changes with the heated wall. With increasing wall temperature, there is a delay in the resolubilization and recrystallization of vaterite into calcite due to lower solubility. That is, in the heated section, the polymorphic transformation does not follow the increase in the mass deposition rate and increase in scale thickness, resulting in a lower proportion between calcite and vaterite.

4. CONCLUSION

The relationship between temperature and the deposition of calcium carbonate could be observed in a series of tests with incompatible brines. The heated test section was able to isolate the effects of the thermal boundary layer, which translated into significantly higher values of deposited mass and scaling thickness when compared to non-heated tests.

The database generated in the present work allows the estimation of the scaling rate as a function of the wall temperature. These results will be further used to validate kinetic and diffusion-reaction models under development in the research group.

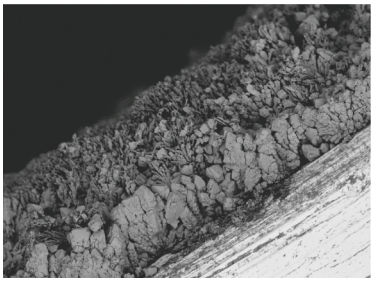

(a) Nonheated (Re = 22800, z = 65m)

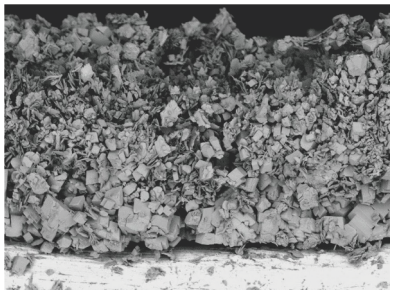

(b) Heated (Re = 22800, z = 65m)

Figure 10: Comparison of the proportion of calcite and vaterite

5. ACKNOWLEDGEMENTS

The authors thank Shell Brazil for financial support and for the permission to publish this paper. The authors also thank all the technical staff of NIDF/UFRJ for the help with the experimental setup and measurements.

6. REFERENCES

Al Omari, M., Rashid, I., Qinna, N., Jaber, A. and Badwan, A., 2016. "Calcium carbonate". *Profiles of drug substances, excipients and related methodology*, Vol. 41, pp. 31–132.

Andritsos, N. and Karabelas, A., 2003. "Calcium carbonate scaling in a plate heat exchanger in the presence of particles". *International Journal of Heat and Mass Transfer*, Vol. 46, No. 24, pp. 4613–4627.

Andritsos, N., Kontopoulou, M., Karabelas, A. and Koutsoukos, P., 1996. "Calcium carbonate deposit formation under isothermal conditions". *The Canadian journal of chemical engineering*, Vol. 74, No. 6, pp. 911–919.

Bots, P., Benning, L.G., Rodriguez-Blanco, J.D., Roncal-Herrero, T. and Shaw, S., 2012. "Mechanistic insights into the crystallization of amorphous calcium carbonate (acc)". *Crystal Growth & Design*, Vol. 12, No. 7, pp. 3806–3814.

Brečević, L. and Nielsen, A.E., 1989. "Solubility of amorphous calcium carbonate". *Journal of crystal growth*, Vol. 98, No. 3, pp. 504–510.

Gargoum, L.A.M., 2018. *Calcium carbonate scale formation under multiphase turbulent conditions*. Ph.D. thesis, University of Leeds.

Incropera, F.P., DeWitt, D.P., Bergman, T.L., Lavine, A.S. *et al.*, 1996. *Fundamentals of heat and mass transfer*, Vol. 6. Wiley New York.

Kawano, J., Shimobayashi, N., Miyake, A. and Kitamura, M., 2009. "Precipitation diagram of calcium carbonate polymorphs: its construction and significance". *Journal of Physics: Condensed Matter*, Vol. 21, No. 42, p. 425102.

Kostoglou, M. and Karabelas, A., 1998. "Comprehensive modeling of precipitation and fouling in turbulent pipe flow". *Industrial & engineering chemistry research*, Vol. 37, No. 4, pp. 1536–1550.

Ogino, T., Suzuki, T. and Sawada, K., 1990. "The rate and mechanism of polymorphic transformation of calcium carbonate in water". *Journal of crystal growth*, Vol. 100, No. 1-2, pp. 159–167.

Rodriguez-Blanco, J.D., Shaw, S. and Benning, L.G., 2011. "The kinetics and mechanisms of amorphous calcium carbonate (acc) crystallization to calcite, via vaterite." *Nanoscale*, Vol. 3, No. 1, pp. 265–271.

Taborek, J., 1997. "Double-pipe and multitube heat exchangers with plain and longitudinal finned tubes". *Heat Transfer Engineering*, Vol. 18, No. 2, pp. 34–45.

Van Santen, R., 1984. "The ostwald step rule". *The Journal of Physical Chemistry*, Vol. 88, No. 24, pp. 5768–5769.

Weyl, P.K., 1959. "The change in solubility of calcium carbonate with temperature and carbon dioxide content". *Geochimica et cosmochimica acta*, Vol. 17, No. 3-4, pp. 214–225.

7. RESPONSIBILITY NOTICE

The authors are solely responsible for the printed material included in this paper.